



Second order nonlinear optics in AlGaAs metasurfaces

Davide Rocco, Luca Carletti, Andrea Locatelli, Andrea Tognazzi, Paolo Franceschini, Marco Gandolfi, Alfonso C. Cino, Giuseppe Leo, Costantino de Angelis

► To cite this version:

Davide Rocco, Luca Carletti, Andrea Locatelli, Andrea Tognazzi, Paolo Franceschini, et al.. Second order nonlinear optics in AlGaAs metasurfaces. *Photoniques*, 2023, 119, pp.46-51. 10.1051/photon/202311946 . hal-04116109

HAL Id: hal-04116109

<https://hal.science/hal-04116109>

Submitted on 3 Jun 2023

HAL is a multi-disciplinary open access archive for the deposit and dissemination of scientific research documents, whether they are published or not. The documents may come from teaching and research institutions in France or abroad, or from public or private research centers.

L'archive ouverte pluridisciplinaire **HAL**, est destinée au dépôt et à la diffusion de documents scientifiques de niveau recherche, publiés ou non, émanant des établissements d'enseignement et de recherche français ou étrangers, des laboratoires publics ou privés.

SECOND ORDER NONLINEAR OPTICS IN AlGaAs METASURFACES

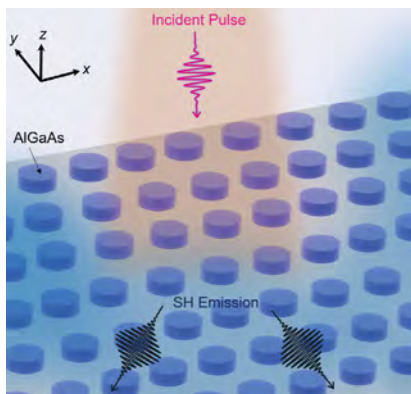
Davide ROCCO^{1,*}, Luca CARLETTI¹, Andrea LOCATELLI¹, Andrea TOGNAZZI², Paolo FRANCESCHINI¹,
Marco GANDOLFI¹, Alfonso C. CINO², Giuseppe LEO³, Costantino DE ANGELIS¹

¹ Department of Information Engineering, University of Brescia, Brescia, Italy

² Department of Engineering, University of Palermo, Palermo, Italy

³ Matériaux et Phénomènes Quantiques, Université Paris Cité, Paris, France

* davide.rocco@unibs.it



Recently, nonlinear optics at the nanoscale level has emerged as a promising branch of nanophotonics. In this work, we focus our attention on Aluminum Gallium Arsenide (AlGaAs) nanoantennas and metasurfaces for efficient and controlled second harmonic photon emission. After a brief introduction concerning the main studies in this field, we present the latest results achieved in AlGaAs platforms both in the lossless and absorption regimes.

<https://doi.org/10.1051/photon/202311946>

This is an Open Access article distributed under the terms of the Creative Commons Attribution License (<http://creativecommons.org/licenses/by/4.0>), which permits unrestricted use, distribution, and reproduction in any medium, provided the original work is properly cited.

In the last years, nano-antennas made of dielectric materials have attracted much attention for the nonlinear generation of light, mainly because of their lower loss with respect to the metallic counterparts. The nonlinear phenomena in Gallium Arsenide (GaAs) and AlGaAs nano-platforms constitute innovative solutions for pioneering researches on phenomena such as Second Harmonic Generation (SHG) in GaAs nanowires, hybrid GaAs plasmonic nano-holes, GaAs micro-ring resonators on insulator and newly, dielectric nano-antennas

and metasurfaces. The AlGaAs success mainly stems from the dependence of its band-gap energy on the alloy composition. Notably, $\text{Al}_x\text{Ga}_{1-x}\text{As}$ presents a direct gap that increases with the Al molar fraction x and permits two-photon-absorption-free operation close to the third communication window ($\sim 1.5 \mu\text{m}$) for $x \geq 0.18$ [1]. Another aspect to underline is that, AlGaAs possess a large non-resonant quadratic susceptibility, $\chi^{(2)}$ (of the order of 200 pm/V for $\text{Al}_{0.18}\text{Ga}_{0.82}\text{As}$ in the near infrared) [2]. All the aforementioned properties highlight the potential of AlGaAs for

achieving efficient second order harmonic generation.

In this work, we present the newest achievements related to SHG in AlGaAs platforms. The manuscript is organized as follow: firstly, we briefly describe the state of the art of these devices and their practical implications by highlighting the main breakthrough studies. Finally, we discuss the opportunity offered by AlGaAs metasurfaces to enlarge the operating working wavelength by exploiting higher order multipoles at the fundamental wavelength that guarantee a sizable SHG efficiency even in the dielectric absorption spectral region.

For the sake of completeness, we underline that, when facing nonlinear generated signals, the SHG efficiency is not the only interesting parameter for optical applications. For instance, a few recent studies have demonstrated that the SH phase control and engineering is fundamental for achieving nonlinear metasurfaces acting as a metalens or with considerable nonlinear beam steering performance [2], therefore increasing the potential applications of AlGaAs meta-devices.

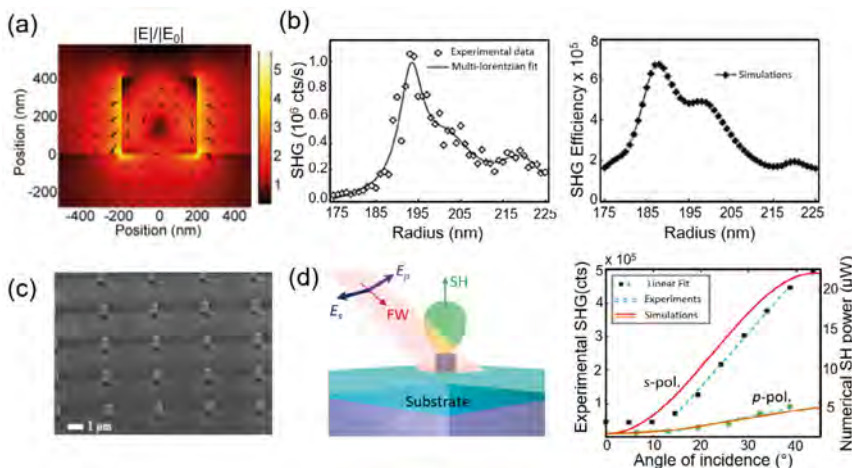
EXPECTED CONTENTS

One of the first theoretical demonstration of the great promise of AlGaAs for nonlinear nanophotonics considered a platform made by isolated cylindrical nanodisk in a homogenous air environment which leads to an individual SHG efficiency of the order of 10^{-3} . The incident excitation, assumed to be a linearly polarized plane wave with intensity, I_0 , of $1\text{GW}/\text{cm}^2$, was in the near-infrared region (1550 nm) in order to excite a magnetic dipolar resonance of the dielectric pillar (radius of 225 nm and height equal to 400 nm). Since AlGaAs belongs to the $3m$ symmetry group and it presents a cubic crystalline structure, the nonlinear currents at the SH frequency can be expressed as: $J_i^{\text{SH}} = i\omega_{\text{SH}}\epsilon_0\chi(2)E_j^{\omega}E_k^{\omega}$ with $i \neq j \neq k$ where ϵ_0 is the dielectric permittivity of

vacuum, ω_{SH} is the SH angular frequency, and $E_{j(k)}$ is the $j(k)$ Cartesian component of the electric field at the pump frequency ω . The SH signal radiated by the dielectric nanocylinder was computed by using such currents as the sources in the numerical calculations at the SH. This breakthrough numerical demonstration was shortly after followed by a laboratory experiment [1]. In this scenario, for manufacturing reasons, the cylindrical pillar was grown over a low refractive index substrate that provokes a reduction of the measured SH efficiency down to 10^{-5} . Let us point out that this value is orders of magnitude higher with respect to the record one reached in plasmonic nanoantennas. In this framework, hybrid metallo-dielectric structures have been deeply investigated [3]. Nevertheless, a lot of efforts [4-6] have also been spent to improve the SHG performance of fully dielectric devices both in terms of nonlinear efficiency and emission directivity as reported in Fig. 1.

More recently, dielectric nanoresonators have been proved to sustain modes with extremely high quality-factor, Q , by demonstrating that an individual AlGaAs nanocylinder can attain high Q supercavity modes which originate from the interference of two similar leaky modes. This mechanism, which is inspired by ●●●

Figure 1. (a) The electric field distribution around the MD resonance and the (b) experimental and simulated SHG efficiency as a function of the pillar radius. (c) SEM image of an AlGaAs cylindrical sample. Adapted with permission from [1] © The Optical Society. (d) The SH directivity toward the normal direction can be increased by tilting the input wavefront.



MULTISPECTRAL LIGHTING SYSTEMS SPECTRUM FIT TO D65 - D50 - A



UP TO 110 CHANNELS
UV 230-400 NM VIS-NIR 400-1000 NM
DIMMING 1-100%

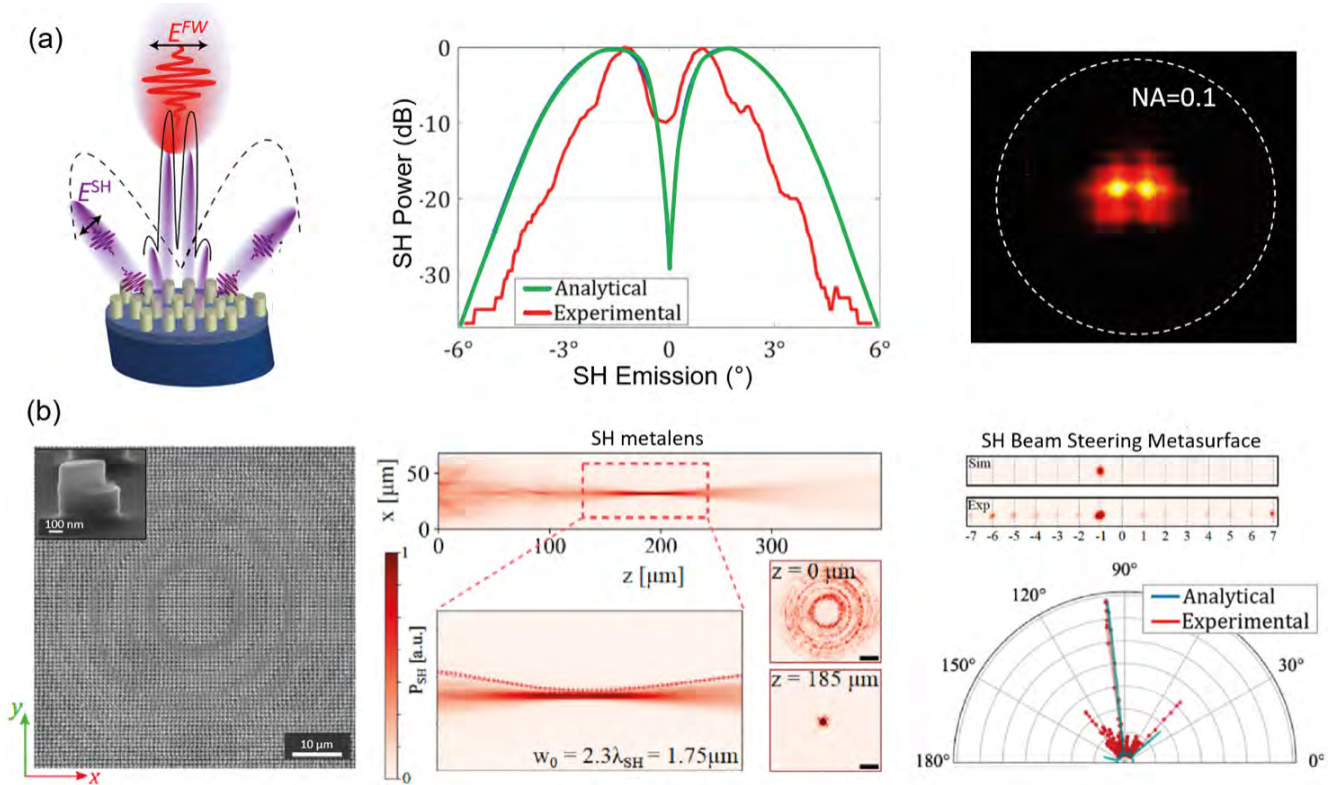


www.ardop.com

**CUSTOM LIGHTING TO MEET YOUR
OWN SPECIFICATIONS AND NEEDS**



+33 5 40 25 05 36
sales@ardop.com



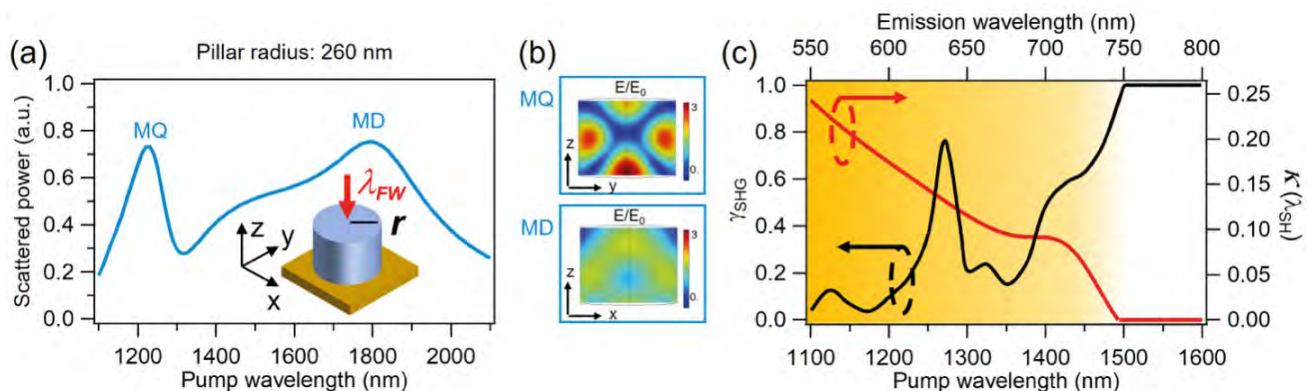
the physical concept known as Bound-state In the Continuum (BIC), is today generally referred to as quasi-BIC [5]. Importantly, it has been proved a huge SHG enhancement when the resonator (an AlGaAs nanodisk) parameters are tuned to the quasi-BIC regime. The obtained SH efficiency surpasses by 2 orders of magnitude the largest one achieved when a magnetic dipolar resonance is excited at the fundamental wavelength. All these concepts, related to the isolated nanoresonator, have been subsequently implemented in nonlinear metasurfaces (*i.e.* structures obtained by properly engineering the spatial repetition of

Figure 2. (a) Analysis of the SHG in an AlGaAs metasurface close to the normal direction. (b) SH metalens and beam steering for AlGaAs metasurface with nano-chair meta-atoms. Adapted with permission from [2] © The Optical Society.

Figure 3. (a) Scattered power as a function of the incident pump wavelength for the pillar with radius 260 nm, height 400 nm. (b) Normalized field distributions at the MQ and MD resonances (c) The γ_{SHG} parameter as a function of the incident wavelength evaluated for the nanodisk with radius of 260 nm (left axis, blue curve) in comparison with the imaginary part of the complex AlGaAs refractive index (right axis, brown curve) as a function of the emission wavelength. Adapted with permission from [7].

the individual pillar) design [2], as summarized in Fig. 2.

In any case, most of the aforementioned solutions are related to the circumstance where either the pump and emission wavelengths are in the lossless region of the nonlinear material that constitutes the metasurface under consideration. Instead, in the following, we exploit the extreme versatility offered by AlGaAs platforms which allows to efficiently operate even beyond the material transparency window. In more details, we reveal that, for an optimized structure, the SH efficiency emitted in the visible part of the electromagnetic spectrum



is comparable, despite the presence of absorption, to the nonlinear second order signal radiated in the near infrared, where no losses occur. Let us consider, as a reference case, an $\text{Al}_{0.18}\text{Ga}_{0.82}\text{As}$ nanodisk with radius r equal to 260 nm and height of 400 nm placed over an AlOx substrate (refractive index ~ 1.6) which is excited by a linearly polarized plane wave excitation with wavelength in between 1100 nm and 2100 nm, I_0 being the incident intensity [7]. The scattered power as a function of the incident wavelength is reported in Fig. 3. Two distinct resonances can be excited: by performing a multipolar decomposition, it is possible to ascribe the one around 1250 nm to a magnetic quadrupole (MQ) and the other to a magnetic dipole (MD). For the considered Al molar fraction x (equal to 0.18), the material losses are non-negligible for wavelengths smaller than 750 nm. Interestingly, for the selected pillar, the MQ resonance is responsible for a SHG signal in the absorption regime whereas the MD resonance is fully lossless, both at the pump and at the SH emitted wavelength, λ_{SH} .

To estimate the impact of losses at λ_{SH} in the nonlinear process of SHG, let us define a parameter $\gamma_{\text{SHG}} = P_{\text{SHG}}[\kappa(\lambda_{\text{SH}})] / P_{\text{SHG}}[\kappa = 0]$. The numerator $P_{\text{SHG}}[\kappa(\lambda_{\text{SH}})]$ is the scattered SH power, and $\kappa(\lambda_{\text{SH}})$ represents the imaginary part of the AlGaAs refractive index at the SH (emission) wavelength. The term $P_{\text{SHG}}[\kappa = 0]$ is the emitted SH power when the absorption at the emission wavelength is factiously turned off. In this computation, the SH power is assumed to be collected by an objective with Numerical Aperture, $\text{NA} = 0.85$. The nonlinear simulations are done following the well-established procedure based on the nonlinear current densities distribution [1] and Fig. 3c reports the obtained results in terms of γ_{SHG} (black line) and the imaginary part of the complex AlGaAs refractive index at the SH wavelength, $\kappa(\lambda_{\text{SH}})$ (red curve).

By definition, when the emission wavelength is greater than 750 nm, the parameter γ_{SHG} is strictly equal to one since κ is set to zero in the implemented AlGaAs refractive index model in this frequency range. Indeed, the

most interesting phenomenon occurs for emission wavelengths lower than 750 nm. In fact, it is possible to observe that, counterintuitively, the γ_{SHG} trend is not only non-inversely proportional to κ but it also presents a maximum peak (equal to 0.75) around 1250 nm, which corresponds to the wavelength at which the excitation resonates with the MQ.

By way of explanation, around the MQ wavelength, the 75% of the potential SH power is effectively radiated thus allowing a sizable SH efficiency which results to be of the order of $5.22 \cdot 10^{-8}$ ($I_0 = 1 \text{ GW/cm}^2$, $\text{NA} = 0.85$). Instead, concerning the MD resonance, for a pump wavelength of 1800 nm, the nonlinear efficiency is equal to $8 \cdot 10^{-8}$ (solely a factor 1.54 higher). This slight decrease is principally attributed to the higher intensity enhancement at the MQ resonance in comparison to the MD. We also note that the considered definition of SH efficiency is the one reported in [1].

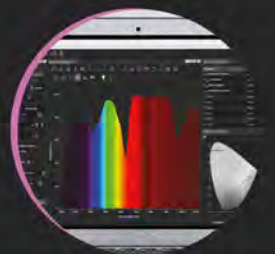
These theoretical predictions are also corroborated by an experimental demonstration. Therefore, we fabricate different AlGaAs nanodisks with radii in the range between 130 nm and 300 nm by obeying the fabrication technique reported in [1]. The implemented measurement set-up is reported in Fig. 4 together with a Scanning Electron Microscope image of one pillar. In the experiments, a fiber laser (Coherent Monaco, 1035 nm wavelength, 1 MHz repetition rate) pumps an optical parametric amplifier (OPA, Coherent Opera-F) that provides a coherent beam with adjustable wavelength in the range 1200-2500 nm. In order to evaluate the radiated SHG power in the presence of losses, in the measurements, we vary the pump wavelength to excite the MQ in the nanodisk. After the interaction with the sample, the reflected beams at fundamental wavelength (FW) and SH are divided by a dichroic mirror [7]. Fig 4b reports a comparison between the numerical calculations and the experimental data for three different pump wavelengths whereas Fig. 4c displays a space-resolved SH intensity map at the incident wavelength of 1250 nm. It is worth noting that the measurements confirm the theoretical ●●●



01 Fiber assemblies & components



02 Optoelectronic systems & lasers



03 Spectroscopy & microscopy



04 Photonics engineering & services



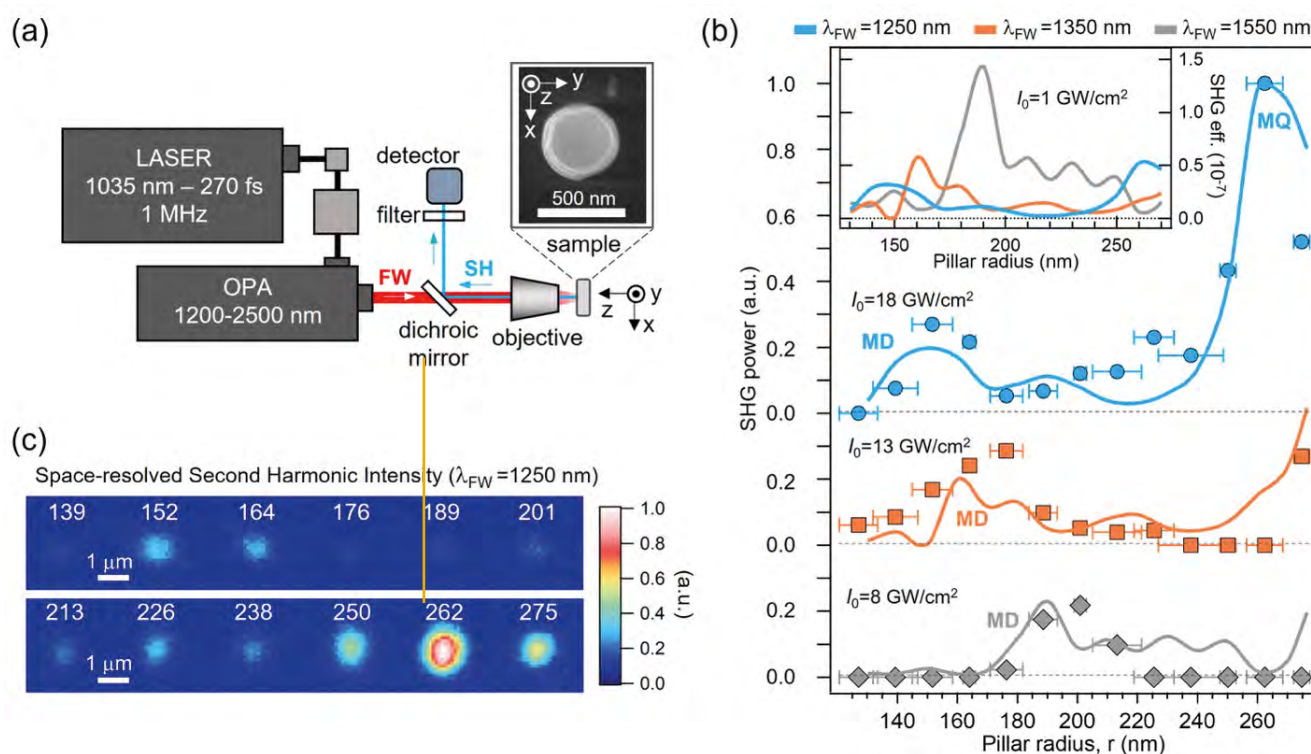


Figure 4. (a) Sketch of the experimental set-up. The inset shows a SEM image of one of the fabricated pillars. (b) Comparison between experimental (markers) and simulated (continuous lines) SHG power as a function of the pillar radius, for three different incident wavelengths and pump intensities. The inset displays the simulated SHG efficiency for a pump with fixed intensity (1 GW/cm^2) at the wavelengths used in the main panel. (c) Space-resolved SH intensity map at the incident wavelength of 1250 nm for the considered pillar radii. Adapted with permission from [7].

predictions and importantly they corroborate the presence of the SH peak around the MQ although the nonlinear signal is partially absorbed. To cover every aspect, the inset of Fig. 4b shows the SHG efficiency for the considered cases assuming the same pump intensity. In any case, the SHG efficiency for the nanodisk with $r = 260 \text{ nm}$ undergoes a limited reduction of a factor of 1.54 when the pump is tuned to the MQ instead of the MD.

The reported results demonstrate the capability of optimized AlGaAs platforms to generate SH signals even in the visible range with a sizable efficiency, with practical implications in different research fields such as nonlinear imaging, holography, and sensing.

CONCLUSION

In this work, we have reported recent achievements on second order nonlinear optics in AlGaAs metasurfaces. In particular, we focus on SHG from nanoantennas where the nonlinear signal is radiated in the dielectric absorption regime. We have demonstrated that by properly exciting a magnetic quadrupolar resonance at the fundamental wavelength (in the

material absorption-less region), it is possible to generate a SH signal in the visible range (with losses) by attaining an harmonic conversion efficiency in the same order of magnitude with respect to magnetic dipolar resonances in the near infrared

region. We believe that the reported results may open new strategies in view of the design of reconfigurable nonlinear metasurfaces exploiting higher order modes to generate harmonic waves far beyond the material transparency window. ●

REFERENCES

- [1] V.F. Gili, L. Carletti, A. Locatelli *et al.*, *Opt. Express* **24**, 15965 (2016)
- [2] C. Gigli, G. Marino, A. Artioli *et al.*, *Optica* **8**, 269 (2021)
- [3] M.C. Larciprete, A. Belardini, M.G. Cappeddu *et al.*, *Phys. Rev. A* **77**, 013809 (2008)
- [4] J.D. Sautter, L. Xu, A. Miroshnichenko *et al.*, *Nano Letters* **19**, 3905 (2019)
- [5] K. Koshelev, A. Bogdanov, Y. Kivshar, *Science* **367**, 288 (2020)
- [6] G. Grinblat, Y. Li, M.P. Nielsen *et al.*, *ACS Nano* **11**, 953 (2017)
- [7] A. Tognazzi, P. Franceschini, D. Rocco *et al.*, *IEEE Photon. Technol. Lett.* (2023).



DISCOVER OUR
PRODUCTS AT
LASERCOMPONENTS.COM
AND RELY ON OUR
EXPERTISE IN PHOTONICS

/ Laser Modules / Laser Diodes / Infrared Components
/ Photodiodes / Fiber Optics / Laser Optics
/ Laser Safety

Discover at
lasercomponents.com

beyond borders